pISSN 2384-1095
eISSN 2384-1109

iMRI 2018;22:71-77

https://doi.org/10.13104/imri.2018.22.1.71

iMRI
Investigative Magnetic Resonance Imaging

Two-Dimensional Image-Based Respiratory Navigator for Free-Breathing Coronary Magnetic Resonance Angiography

Taehoon Shin

Division of Mechanical and Biomedical Engineering, Ewha Womans University, Seoul, Korea

Technical Note

Received: August 21, 2017
Revised: October 7, 2017
Accepted: November 5, 2017

Correspondence to:
Taehoon Shin, Ph.D.
Division of Mechanical and Biomedical Engineering,
Ewha Womans University, 52 Ewhayeodae-gil, Seodaemun-gu,
Seoul 03760, Korea.
Tel. +82-2-3277-6534
Fax. +82-2-3577-3535
E-mail: taehoons@ewha.ac.kr

Purpose: To develop a two-dimensional (2D) image-based respiratory motion correction technique for free-breathing coronary magnetic resonance angiography (MRA).

Materials and Methods: The proposed respiratory navigator obtained aliased a 2D sagittal image from under-sampled k-space data and utilized motion correlation between the aliased images. The proposed navigator was incorporated into the conventional coronary MRA sequence including the diaphragm navigator and tested in three healthy subjects.

Results: The delineation of major coronary arteries was significantly improved using the proposed 2D motion correction (S/I and A/P) compared to one-dimensional (S/I) correction using the conventional diaphragm navigator.

Conclusion: The 2D image-based respiratory navigator was proposed for free-breathing coronary angiography and showed the potential for improving respiratory motion correction compared to the conventional 1D correction.

Keywords: Motion correction; Respiratory navigator; Coronary angiography

INTRODUCTION

While the catheter-based X-ray angiogram is the gold standard for diagnosis of coronary artery disease, coronary magnetic resonance angiography (MRA) has long been sought as an alternative due to its non-invasive and non-toxic nature. Earlier MR approaches employed targeted volume acquisition of each coronary territory using a thin imaging slab, but this tended to produce inconsistent performance depending on the operator skill of coronary localization (1). Whole-heart coronary MRA has been mainly explored which acquires a three-dimensional (3D) volumetric image of entire heart using an axially oriented thick imaging slab. This approach involves minimal level of localization complexity, and provides huge flexibility of post-analysis of 3D data through arbitrary display views (2, 3).

Due to the need for high-resolution 3D encoding, whole heart coronary MRA needs to be performed during free-breathing, which necessitates estimation and correction for respiratory motion. The most established respiratory navigator employs one-dimensional (1D) projection signal from pencil-beam excitation of the diaphragm, which can be

translated to the heart's motion based on empirically known correlation between the two organs (4, 5). However, many studies have found sources of inaccuracy of the diaphragm navigator, such as subject-dependent motion correlation between the diaphragm and heart, and hysteresis during a respiratory cycle (5–8). Also, consideration of superior-inferior (S/I) motion only may not be sufficient in subjects who exhibit significant motions in the other directions.

Direct motion estimation from the heart has been actively explored in recent years due to its potential for more accurate motion estimation than the diaphragm-based navigator. Stehning et al. (3) first introduced the use of 1D S/I projection signal of the heart using a modified 3D radial k-space trajectory. Recently, Lai et al. (9, 10) developed acquisition of outer volume-free projection signals using cosine-modulation along the anterior-posterior (A/P) direction, and extended it to multidimensional estimation by adding motion encoding gradients. While these studies reported significant improvement over the diaphragm navigator, the fact that fine anatomical structures are lost in projected signals leaves a room for further improvement in the accuracy of motion estimation.

Ideally, motion can be best estimated by calculating correlation between fully encoded images which preserves anatomical features and also allows easy separation of the heart from stationary regions (e.g., chest wall). However, such image-based navigator would be impractical due to long acquisition time for full k-space sampling with reasonably high spatial resolution.

In this article, we present a simple image-based respiratory navigator with significantly reduced acquisition time by using under-sampled k-space data instead of fully sampled data. The feasibility of the proposed method was tested by 2D motion correction (S/I and A/P) for free-breathing coronary MRA using phantom and *in-vivo* experiments.

MATERIALS AND METHODS

Motion Estimation between Aliased Images

The proposed motion estimation is based on the fact that translational motion correlation is preserved in aliased images from evenly under-sampled k-space data. This concept is illustrated in Figure 1; six-fold aliased images of a resolution phantom at a reference position (a) are shifted along the S/I direction (b). The corresponding full-field of view (FOV) images are shown at the upper right corner. Apparently, the second full-FOV image is a shifted version (16 mm in the S/I direction) of the reference full-FOV image. Likewise, each of six replicas in the second aliased images is displaced by the same direction and distance with

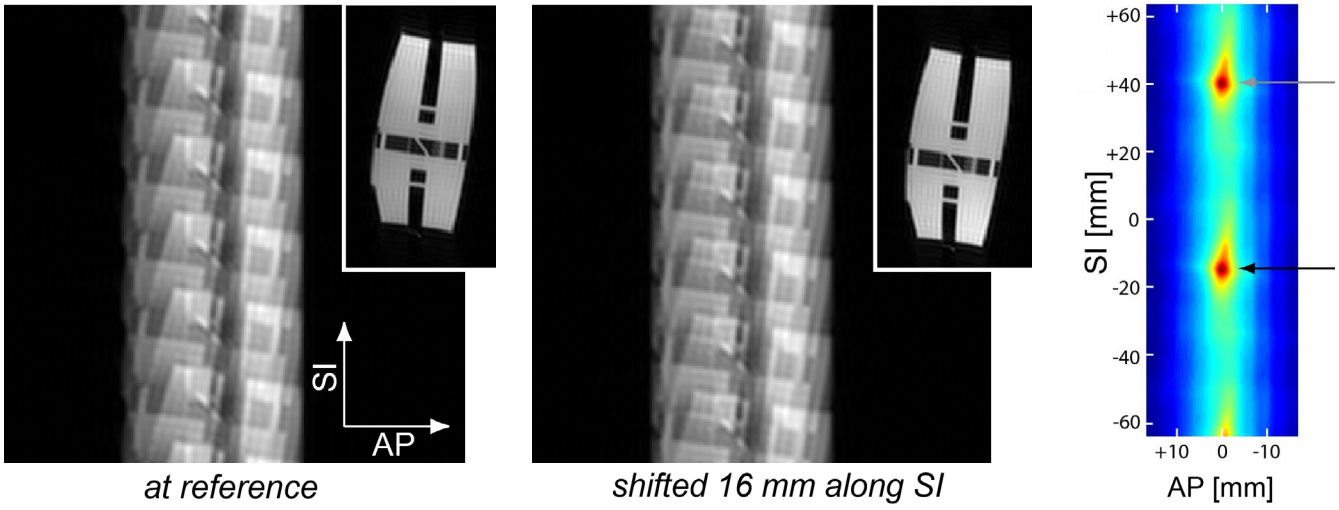

Fig. 1. Illustration of the proposed 2D motion estimation. (a) Six-fold aliased image of the resolution phantom (a): at a reference position, (b) Shifted 16 mm along the SI direction. (c) Correlation between the reference aliased image and the second aliased image shifted over 2D search space. Due to the same translations of the six replicas, a local maximum is yielded at the true displacement (black arrow), and also at increments of (n·FOV/R) (gray arrow) away from the true solution (n = integer, R = under-sampling rate).

respect to the reference aliased image. Thus, the second aliased image that is simply summation of the six replicas, is also a shifted version of the reference aliased image.

Figure 1c shows the correlation between the reference aliased image and the second aliased image shifted over 2D search space, as measured by mean square error between the two images multiplied by minus one. The correlation has a local maximum when the second image is shifted back by 16 mm in the S/I direction, which represents the true solution (black arrow). With an under-sampling rate of *R*, the same local maximum is also yielded at increments of (n FOV/R) away from the true solution in the phase encoding direction (gray arrow). To avoid this ambiguity, *R* must be chosen such that the expected range of true displacement is less than (FOV/R).

Phantom and *in-vivo* Experiments

All experiments were performed on a GE 1.5T Signa MR scanner equipped with maximum gradient amplitude of 40 mT/m and slew rate of 150 mT/m/ms and 8-channel cardiac array coil for signal reception. Phantom experiments were performed to test the accuracy of the aliased image-based motion estimation. Sagittal images were obtained from a resolution phantom placed at nine S/I positions in 4 mm increments by moving the scanner table (i.e., S16, S12, S8, S4, S0, I4, I8, I12, and I16 mm with respect to the iso-center). The under-sampling rate *R* varied from 1 (full sampling) to 8. Imaging parameter included radiofrequency (RF)-spoiled gradient echo (GRE) readout, spatial resolution = 3.3 × 3.3 mm^2, FA = 15°, slice thickness = 12 mm, and TR = 2.7 ms. With the iso-center image as reference, motion was searched iteratively using the least-square criterion.

While the actual motion occurred along the S/I direction only, motion estimation was performed over 2D search space to investigate errors in both S/I and A/P directions. Search range was [-16.4, 16.4] mm along the S/I direction and [-6.6, 6.6] mm along the A/P direction with a step size of 0.4 mm (1/8 pixel). For the sub-pixel matching, the phantom images were interpolated through zero-padding in k-space by factor of 8, and shifted around in the interpolated image domain.

The pulse sequence for *in vivo* coronary MRA consisted of T2-prep (11), diaphragm navigator acquisition, fat saturation and coronary data acquisition followed by notched saturation and image-based navigator acquisition (Fig. 2). This is the same as a commonly used whole-heart MRA sequence, except for the proposed image-based navigator after the coronary acquisition. The phase encoding for the image-based navigator was set to the S/I direction so that chest wall could be easily excluded from a region-of-interest (ROI) for motion search (Fig. 3). Notched saturation with a notch-width of 28 cm was also applied along the S/I direction for suppression of thoracic trunk signal outside the FOV. A so-called sandwich design (180 degree hard pulse between halves of slice-selective pulse) was used, which is fast and robust to off-resonance (12).

Free-breathing coronary MRA was performed in three healthy volunteers with imaging parameters including imaging orientation = axial, 3DFT balanced SSFP readout, FOV = 26 × 26 × 14 cm^3, spatial resolution = 1.3 × 1.3 × 1.6 mm^3, 24 view per segment, FA = 80°, TR = 4.2 ms, acquisition time = 100.8 ms, and total scan time = 702 heart beats. Imaging parameters for the 2D navigator included imaging orientation = sagittal, 2DFT GRE readout, FOV = 32 × (32/R) cm^2 with R = 6, spatial resolution = 3.8 × 3.8 mm^2, FA = 25°, slice thickness = 15 mm, TR = 2.8 ms, and acquisition time = 39.2 ms. A full-FOV sagittal image was acquired over six cardiac cycles before the coronary MRA and used for ROI specification (Fig. 3a). 2D motion search was performed for the MRA data from the rest of cardiac cycles using the least-square correlation metric. Aliased images for navigator were reconstructed

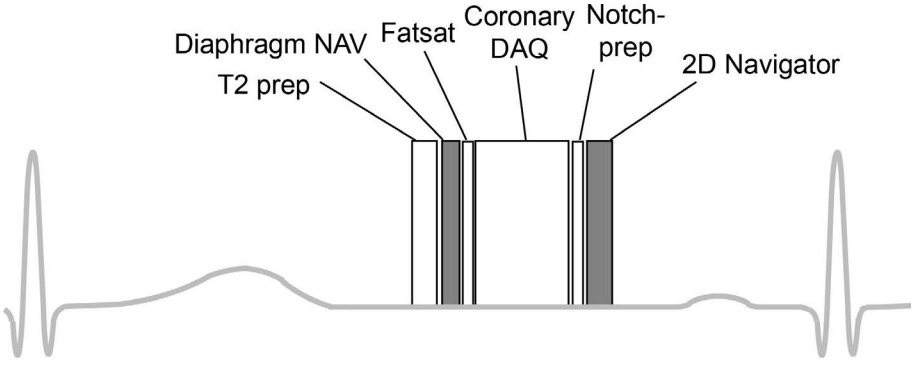

Fig. 2. Timing diagram of coronary MRA with diaphragm navigator and 2D image-based navigator. The sequence consisted of a T2-preparation pulse, diaphragm navigator acquisition, fat saturation pulse, coronary acquisition, notched saturation pulse, and 2D image-based navigator acquisition, sequentially.

using signals from the anterior coil elements only since posterior elements receive signal mostly from the back while only little from the heart. Search range was [-19.0, 19.0] mm along the S/I direction and [-7.6, 7.6] mm along the A/P direction with a step size of 0.48 mm (1/8 pixel). For comparison, 1D S/I motion was estimated using the projection signal from the diaphragm and a correlation factor of 0.6 (5).

RESULTS

Exemplary aliased phantom images obtained at the iso-center and at a 16-cm inferior location are shown in Figure 1. Table 1 summarizes the motion estimation error of the phantom experiment, where each cell contains errors in x- and y-directions (in millimeters) for specific location and under-sampling factor. The absolute errors of motion estimation in the phantom test were 0.20 ± 0.16 mm, 0.22 ± 0.13 mm, 0.28 ± 0.14 mm, 0.32 ± 0.10 mm, and 0.38 ± 0.11 mm for under-sampling rate of 1, 2, 4, 6, and 8, respectively (Table 1). The estimation errors increased slightly with the under-sampling rate, due to decreasing SNR. Compared to the error from fully sampled data, additional errors due to k-space under-sampling were negligible, validating the motion correlation between aliased images. The non-zero

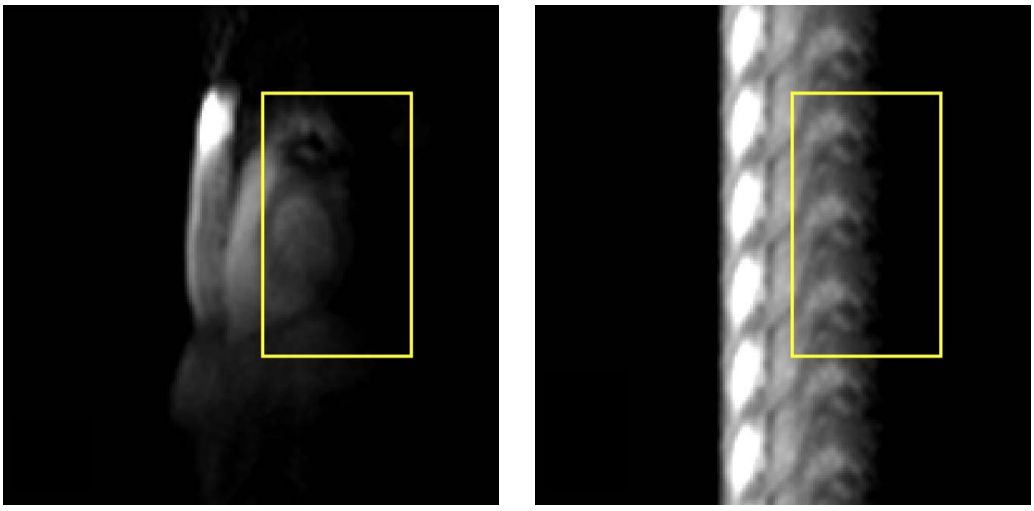

a b

Fig. 3. (a) Full-FOV sagittal image was acquired prior to coronary MRA scan and used to specify an ROI for motion estimation (yellow box). (b) Six-fold aliased image acquired during an MRA scan clearly shows image features to be used for motion estimation.

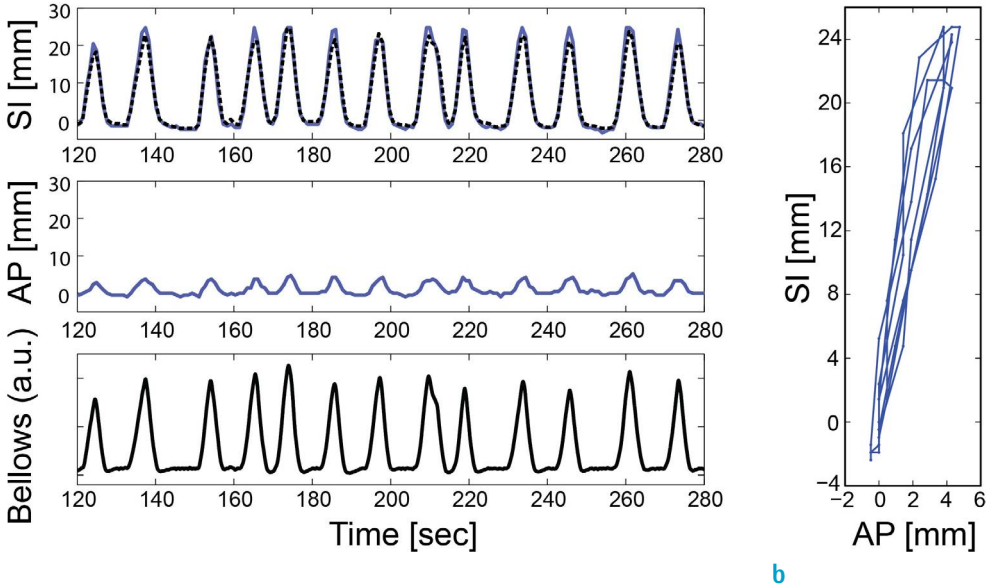

a b

Fig. 4. (a) Estimated motion in the S/I and A/P directions (in millimeters) and bellows signal (in arbitrary unit denoted as 'a.u.'). In the top row, blue solid curve and black dotted curve represents the estimates by the proposed image-based navigator and the diaphragm navigator, respectively. (b) Trajectory of estimated motion in the SI-AP plane.

error from the fully sampled data was presumably due to errors of frequency and phase encoding gradients, which caused inaccurate spatial resolution of reconstructed images.

Figure 3 depicts an *in vivo* full-FOV image used for ROI specification (yellow box), and a six-fold aliased image acquired during an MRA scan. The aliased image exhibits sufficient image features to be used for motion estimation.

Figure 4a depicts estimated respiratory motions using the proposed 2D navigator (solid blue) and 1D diaphragm

Table 1. Motion Estimation Errors of Phantom Experiments

R	S16 cm	S12 cm	S8 cm	S4 cm	I4 cm	I8 cm	I12 cm	I16 cm	Abs (error)
1	0.0 0.33	0.0 0.04	0.0 0.16	0.0 0.08	0.0 -0.08	0.0 -0.16	0.0 -0.24	0.0 -0.53	0.20 ± 0.16
2	0.0 0.33	0.0 0.24	0.0 0.16	0.0 0.08	0.0 -0.08	0.0 -0.16	0.0 -0.45	0.21 -0.12	0.22 ± 0.13
4	-0.21 0.33	0.0 0.24	0.0 0.16	0.0 0.08	0.0 -0.29	0.0 -0.16	0.21 -0.45	0.21 -0.33	0.28 ± 0.14
6	-0.21 0.12	-0.21 0.24	0.0 0.16	0.0 0.29	0.0 -0.29	0.0 -0.37	0.21 -0.45	0.21 -0.33	0.32 ± 0.10
8	-0.21 0.33	-0.21 0.45	0.0 0.37	0.0 0.29	0.0 -0.29	0.0 -0.37	0.0 -0.24	0.21 -0.53	0.38 ± 0.11

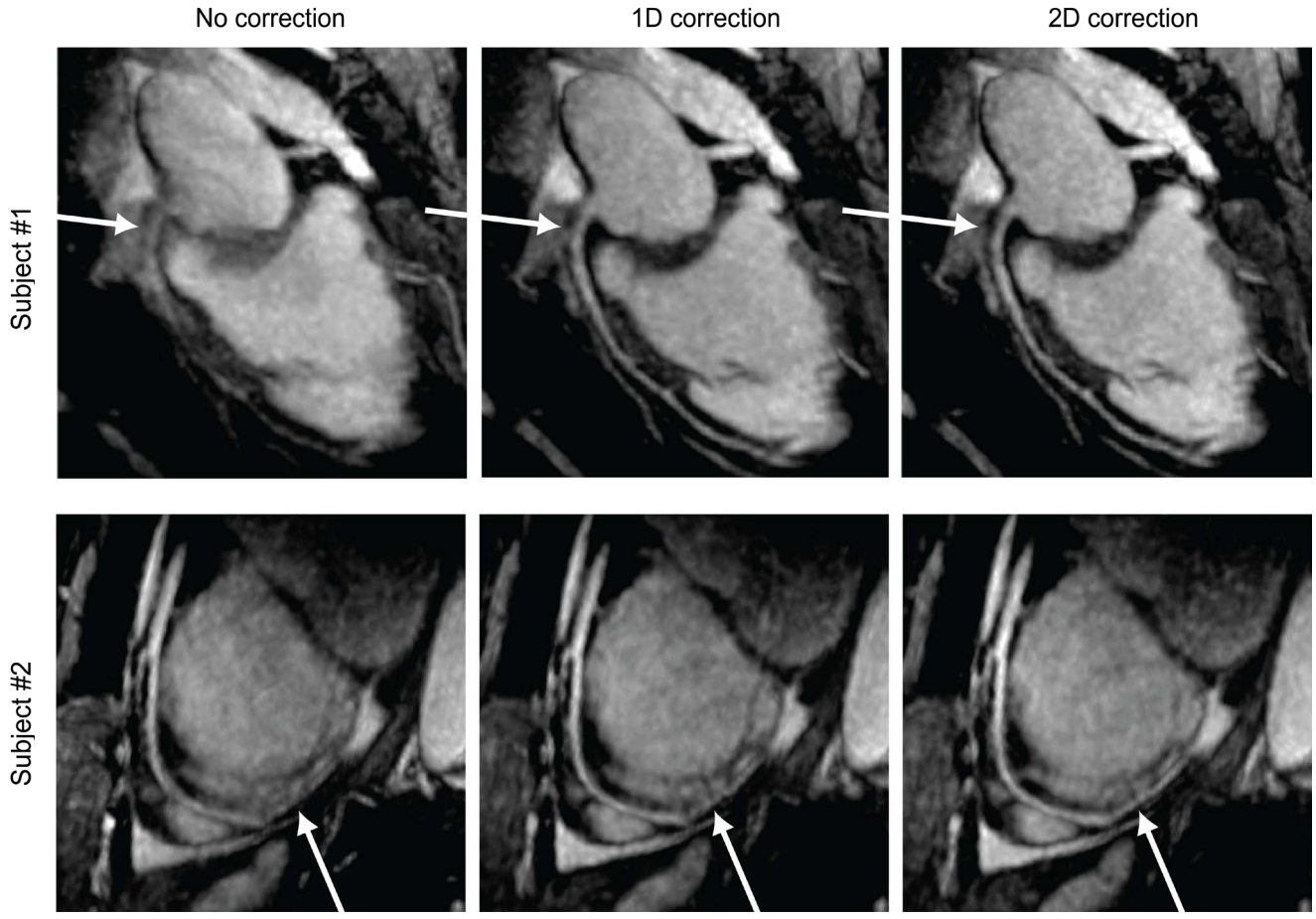

Fig. 5. Representative coronary MRA images obtained using no correction (left column), 1D correction (S/I) based on the diaphragm navigator (middle row) and 2D correction (S/I + A/P) based on the proposed image-based navigator (right column). The delineation of the arterial tree progressively improves with the 1D and 2D corrections (arrows).

navigator (dotted black) in a time segment of 120–280 second, temporally synchronized with the signal recorded from respiratory bellows (solid black). Good agreement between S/I motions estimated by the diaphragm navigator and the image-based navigator was shown. Figure 4b depicts 2D trace of estimated motion using the proposed method in a time segment of 160–200 sec, showing hysteresis between inspiration and expiration.

Figure 5 shows representative MRA images obtained using no correction (left), 1D correction based on the diaphragm navigator (middle), and 2D correction based on the proposed image-based navigator (right). The total scan time for the two subjects ranged from 10–12 min. The depiction of RCA (top row) and LAD (bottom row) arteries substantially improved with the 1D correction in the S/I direction. The additional improvement with 2D correction was observed especially in the delineation of the distal LAD in the 2nd subject (arrow in the bottom row).

DISCUSSION

Image-based navigators are advantageous over projection-based methods due to improved preservation of image features, capability of multi-dimensional estimation, and easy separation of the heart from other neighboring organs. However, acquiring full-FOV images requires a long acquisition time, which would generate errors caused by motion artifacts and temporal delay to the coronary acquisition. The proposed method overcomes this issue by utilizing motion correlation between aliased images that can be acquired using a significantly shortened acquisition window. The feasibility of the aliased image-based navigator was demonstrated by 2D respiratory motion correction for free-breathing coronary MRA. Using six-fold accelerated acquisition, the proposed method corrected for S/I and A/P motions, and resulted in improved depiction of arteries compared with the diaphragm navigator.

Under-sampling rate R for the image-based navigator should be chosen based on the trade-off involved. If the under-sampling rate is too low, the image-based navigator may suffer from motion artifacts due to long acquisition window. If the under-sampling rate is too high, the maximum detectable displacement (FOV/R) is reduced. With an expected maximum S/I displacement of ~2 cm and an S/I FOV of 32 cm, the maximum possible under-sampling rate appears to be 16. However, another issue with too high R is low SNR which degrades the accuracy of motion estimation. While the empirically chosen R = 6 has yielded promising initial results in this study, further optimization is warranted in a large cohort of subjects.

The 2D image-based navigator was used for estimating motions along the S/I and A/P directions which are believed to be two dominant axes for respiratory motion. Although depiction of arteries was improved compared with the diaphragm navigator in our study, the uncorrected L/R direction may not be negligible, depending on subjects (10, 13). Thus, it may be worthwhile to investigate the extension of the technique to 3D motion estimation. One easy implementation would be addition of another image-based navigator on an axial plane immediately before the coronary acquisition instead of the diaphragm navigator. Axially oriented images will be able to estimate motions along the A/P and L/R directions, and can be combined with S/I and A/P motions estimated by sagittal images.

In summary, we propose a new image-based respiratory navigator for free-breathing coronary angiography and demonstrate its feasibility in healthy subjects. The proposed approach utilizes the preservation of motion correlation between aliased images, allowing for rapid and accurate estimation of 2D motion. The proposed 2D correction has shown to improve the depiction of the arteries compared to the conventional diaphragm-based 1D correction.

Acknowledgements

This work was supported by Ewha Womans University research grant of 2017, Advanced MR Study Group, Korean Society of Magnetic Resonance in Medicine, 2017, and NIH/NIBIB research grant (R21EB019206).

REFERENCES

1. Stuber M, Weiss RG. Coronary magnetic resonance angiography. J Magn Reson Imaging 2007;26:219-234
2. Chiribiri A, Ishida M, Nagel E, Botnar RM. Coronary imaging with cardiovascular magnetic resonance: current state of the art. Prog Cardiovasc Dis 2011;54:240-252
3. Stehning C, Bornert P, Nehrke K, Eggers H, Stuber M. Free-breathing whole-heart coronary MRA with 3D radial SSFP and self-navigated image reconstruction. Magn Reson Med 2005;54:476-480
4. Danias PG, McConnell MV, Khasgiwala VC, Chuang ML, Edelman RR, Manning WJ. Prospective navigator correction of image position for coronary MR angiography. Radiology 1997;203:733-736
5. Danias PG, Stuber M, Botnar RM, Kissinger KV, Edelman

RR, Manning WJ. Relationship between motion of coronary arteries and diaphragm during free breathing: lessons from real-time MR imaging. AJR Am J Roentgenol 1999;172:1061-1065
6. Nehrke K, Bornert P, Manke D, Bock JC. Free-breathing cardiac MR imaging: study of implications of respiratory motion--initial results. Radiology 2001;220:810-815
7. Taylor AM, Keegan J, Jhooti P, Firmin DN, Pennell DJ. Calculation of a subject-specific adaptive motion-correction factor for improved real-time navigator echo-gated magnetic resonance coronary angiography. J Cardiovasc Magn Reson 1999;1:131-138
8. Keegan J, Gatehouse P, Yang GZ, Firmin D. Coronary artery motion with the respiratory cycle during breath-holding and free-breathing: implications for slice-followed coronary artery imaging. Magn Reson Med 2002;47:476-481
9. Lai P, Larson AC, Bi X, Jerecic R, Li D. A dual-projection respiratory self-gating technique for whole-heart coronary MRA. J Magn Reson Imaging 2008;28:612-620
10. Lai P, Bi X, Jerecic R, Li D. A respiratory self-gating technique with 3D-translation compensation for free-breathing whole-heart coronary MRA. Magn Reson Med 2009;62:731-738
11. Brittain JH, Hu BS, Wright GA, Meyer CH, Macovski A, Nishimura DG. Coronary angiography with magnetization-prepared T2 contrast. Magn Reson Med 1995;33:689-696
12. Cunningham CH, Lustig M, Hu BS, et al. Novel design for notched RF saturation pulses using the SLR transform. In Proceedings of the 15th Scientific Meeting of International Society for Magnetic Resonance in Medicine. Berlin, 2007:1709
13. Manke D, Nehrke K, Bornert P, Rosch P, Dossel O. Respiratory motion in coronary magnetic resonance angiography: a comparison of different motion models. J Magn Reson Imaging 2002;15:661-671